Rapid Communications

Study of $e^+e^- \to \pi^+\pi^-\pi^0\eta_c$ and evidence for $Z_c(3900)^\pm$ decaying into $\rho^\pm\eta_c$

M. Ablikim,[1] M. N. Achasov,[10,d] S. Ahmed,[15] M. Albrecht,[4] M. Alekseev,[55a,55c] A. Amoroso,[55a,55c] F. F. An,[1] Q. An,[52,42] Y. Bai,[41] O. Bakina,[27] R. Baldini Ferroli,[23a] Y. Ban,[35,k] K. Begzsuren,[25] D. W. Bennett,[22] J. V. Bennett,[5] N. Berger,[26] M. Bertani,[23a] D. Bettoni,[24a] F. Bianchi,[55a,55c] I. Boyko,[27] R. A. Briere,[5] H. Cai,[57] X. Cai,[1,42] A. Calcaterra,[23a] G. F. Cao,[1,46] S. A. Cetin,[45b] J. Chai,[55c] J. F. Chang,[1,42] W. L. Chang,[1,46] G. Chelkov,[27,b,c] G. Chen,[1] H. S. Chen,[1,46] J. C. Chen,[1] M. L. Chen,[1,42] P. L. Chen,[53] S. J. Chen,[33] Y. B. Chen,[1,42] W. Cheng,[55c] G. Cibinetto,[24a] F. Cossio,[55c] H. L. Dai,[1,42] J. P. Dai,[37,h] A. Dbeyssi,[15] D. Dedovich,[27] Z. Y. Deng,[1] A. Denig,[26] I. Denysenko,[27] M. Destefanis,[55a,55c] F. De Mori,[55a,55c] Y. Ding,[31] C. Dong,[34] J. Dong,[1,42] L. Y. Dong,[1,46] M. Y. Dong,[1,42,46] Z. L. Dou,[33] S. X. Du,[60] P. F. Duan,[1] J. Z. Fan,[44] J. Fang,[1,42] S. S. Fang,[1,46] Y. Fang,[1] R. Farinelli,[24a,24b] L. Fava,[55b,55c] F. Feldbauer,[4] G. Felici,[23a] C. Q. Feng,[52,42] M. Fritsch,[4] C. D. Fu,[1] Y. Fu,[1] X. L. Gao,[52,42] Y. Gao,[44] Y. G. Gao,[6] Z. Gao,[52,42] I. Garzia,[24a,24b] A. Gilman,[49] K. Goetzen,[11] L. Gong,[34] W. X. Gong,[1,42] W. Gradl,[26] M. Greco,[55a,55c] L. M. Gu,[33] M. H. Gu,[1,42] S. Gu,[2] Y. T. Gu,[13] A. Q. Guo,[1,22] L. B. Guo,[32] R. P. Guo,[1,46] Y. P. Guo,[26] A. Guskov,[27] Z. Haddadi,[29] S. Han,[57] X. Q. Hao,[16] F. A. Harris,[47] K. L. He,[1,46] F. H. Heinsius,[4] T. Held,[4] Y. K. Heng,[1,42,46] T. Holtmann,[4] Z. L. Hou,[1] H. M. Hu,[1,46] J. F. Hu,[37,h] T. Hu,[1,42,46] Y. Hu,[1] G. S. Huang,[52,42] J. S. Huang,[16] X. T. Huang,[36] X. Z. Huang,[33] N. Huesken,[50] T. Hussain,[54] W. Ikegami Andersson,[56] M. Irshad,[52,42] Q. Ji,[1] Q. P. Ji,[16] X. B. Ji,[1,46] X. L. Ji,[1,42] H. B. Jiang,[36] X. S. Jiang,[1,42,46] X. Y. Jiang,[34] J. B. Jiao,[36] Z. Jiao,[18] D. P. Jin,[1,42,46] S. Jin,[33] Y. Jin,[48] T. Johansson,[56] A. Julin,[49] N. Kalantar-Nayestanaki,[29] X. S. Kang,[34] M. Kavatsyuk,[29] B. C. Ke,[1] I. K. Keshk,[4] T. Khan,[52,42] A. Khoukaz,[50] P. Kiese,[26] R. Kiuchi,[1] R. Kliemt,[11] L. Koch,[28] O. B. Kolcu,[45b,f] B. Kopf,[4] M. Kuemmel,[4] M. Kuessner,[4] A. Kupsc,[56] W. Kühn,[28] J. S. Lange,[28] P. Larin,[15] L. Lavezzi,[55c] S. Leiber,[4] H. Leithoff,[26] C. Leng,[55c] C. Li,[56] Cheng Li,[52,42] D. M. Li,[60] F. Li,[1,42] G. Li,[1] H. B. Li,[1,46] H. J. Li,[1,46] J. C. Li,[1] J. W. Li,[40] Ke Li,[1] Lei Li,[3] P. L. Li,[52,42] P. R. Li,[46,7] Q. Y. Li,[36] T. Li,[36] W. D. Li,[1,46] W. G. Li,[1] X. L. Li,[36] X. N. Li,[1,42] X. Q. Li,[34] Z. B. Li,[43] H. Liang,[52,42] Y. F. Liang,[39] Y. T. Liang,[28] G. R. Liao,[12] L. Z. Liao,[1,46] J. Libby,[21] C. X. Lin,[43] D. X. Lin,[15] B. Liu,[37,h] B. J. Liu,[1] C. X. Liu,[1] D. Liu,[52,42] D. Y. Liu,[37,h] F. H. Liu,[38] Fang Liu,[1] Feng Liu,[6] H. B. Liu,[13] H. J. Liu,[41] H. M. Liu,[1,46] Huanhuan Liu,[1] Huihui Liu,[17] J. B. Liu,[52,42] J. Y. Liu,[1,46] K. Y. Liu,[31] Ke Liu,[6] Q. Liu,[46] S. B. Liu,[52,42] X. Liu,[30] Y. B. Liu,[34] Z. A. Liu,[1,42,46] Zhiqing Liu,[26] Y. F. Long,[35,k] X. C. Lou,[1,42,46] H. J. Lu,[18] J. D. Lu,[1,46] J. G. Lu,[1,42] Y. Lu,[1] Y. P. Lu,[1,42] C. L. Luo,[32] M. X. Luo,[59] P. W. Luo,[43] T. Luo,[9,i] X. L. Luo,[1,42] S. Lusso,[55c] X. R. Lyu,[46] F. C. Ma,[31] H. L. Ma,[1] L. L. Ma,[36] M. M. Ma,[1,46] Q. M. Ma,[1] X. N. Ma,[34] X. X. Ma,[1,46] X. Y. Ma,[1,42] Y. M. Ma,[36] F. E. Maas,[15] M. Maggiora,[55a,55c] S. Maldaner,[26] Q. A. Malik,[54] A. Mangoni,[23b] Y. J. Mao,[35,k] Z. P. Mao,[1] S. Marcello,[55a,55c] Z. X. Meng,[48] J. G. Messchendorp,[29] G. Mezzadri,[24a] J. Min,[1,42] T. J. Min,[33] R. E. Mitchell,[22] X. H. Mo,[1,42,46] Y. J. Mo,[6] C. Morales Morales,[15] N. Yu. Muchnoi,[10,d] H. Muramatsu,[49] A. Mustafa,[4] S. Nakhoul,[11,g] Y. Nefedov,[27] F. Nerling,[11,g] I. B. Nikolaev,[10,d] Z. Ning,[1,42] S. Nisar,[8,j] S. L. Niu,[1,42] S. L. Olsen,[46] Q. Ouyang,[1,42,46] S. Pacetti,[23b] Y. Pan,[52,42] M. Papenbrock,[56] P. Patteri,[23a] M. Pelizaeus,[4] H. P. Peng,[52,42] K. Peters,[11,g] J. Pettersson,[56] J. L. Ping,[32] R. G. Ping,[1,46] A. Pitka,[4] R. Poling,[49] V. Prasad,[52,42] H. R. Qi,[2] M. Qi,[33] T. Y. Qi,[2] S. Qian,[1,42] C. F. Qiao,[46] N. Qin,[57] X. S. Qin,[4] Z. H. Qin,[1,42] J. F. Qiu,[1] S. Q. Qu,[34] K. H. Rashid,[54] K. Ravindran,[21] C. F. Redmer,[26] M. Richter,[4] A. Rivetti,[55c] M. Rolo,[55c] G. Rong,[1,46] Ch. Rosner,[15] M. Rump,[50] A. Sarantsev,[27,e] M. Savrié,[24b] C. Schnier,[4] K. Schoenning,[56] W. Shan,[19] X. Y. Shan,[52,42] M. Shao,[52,42] C. P. Shen,[2] P. X. Shen,[34] X. Y. Shen,[1,46] H. Y. Sheng,[1] X. Shi,[1,42] J. J. Song,[36] W. M. Song,[36] X. Y. Song,[1] S. Sosio,[55a,55c] C. Sowa,[4] S. Spataro,[55a,55c] F. F. Sui,[36] G. X. Sun,[1] J. F. Sun,[16] L. Sun,[57] S. S. Sun,[1,46] Y. J. Sun,[52,42] Y. K. Sun,[52,42] Y. Z. Sun,[1] Z. J. Sun,[1,42] Z. T. Sun,[1] Y. X. Tan,[52,42] C. J. Tang,[39] G. Y. Tang,[1] X. Tang,[1] M. Tiemens,[29] B. Tsednee,[25] I. Uman,[45d] B. Wang,[1] B. L. Wang,[46] C. W. Wang,[33] D. Y. Wang,[35,k] H. H. Wang,[36] K. Wang,[1,42] L. L. Wang,[1] L. S. Wang,[1] M. Wang,[36] Meng Wang,[1,46] P. Wang,[1] P. L. Wang,[1] W. P. Wang,[52,42] X. F. Wang,[1] Y. Wang,[52,42] Y. D. Wang,[15] Y. F. Wang,[1,42,46] Z. Wang,[1,42] Z. G. Wang,[1,42] Z. Y. Wang,[1] Zongyuan Wang,[1,46] T. Weber,[4] D. H. Wei,[12] P. Weidenkaff,[26] S. P. Wen,[1] U. Wiedner,[4] M. Wolke,[56] L. H. Wu,[1] L. J. Wu,[1,46] Z. Wu,[1,42] L. Xia,[52,42] X. Xia,[36] D. Xiao,[1] Y. J. Xiao,[1,46] Z. J. Xiao,[32] Y. G. Xie,[1,42] Y. H. Xie,[6] X. A. Xiong,[1,46] Q. L. Xiu,[1,42] G. F. Xu,[1] J. J. Xu,[1,46] L. Xu,[1] Q. J. Xu,[14] X. P. Xu,[40] F. Yan,[53] L. Yan,[55a,55c] W. B. Yan,[52,42] W. C. Yan,[2] H. J. Yang,[37,h] H. X. Yang,[1] L. Yang,[57] R. X. Yang,[52,42] S. L. Yang,[1,46] Y. H. Yang,[33] Y. X. Yang,[12] Yifan Yang,[1,46] M. Ye,[1,42] M. H. Ye,[7] J. H. Yin,[1] Z. Y. You,[43] B. X. Yu,[1,42,46] C. X. Yu,[34] J. S. Yu,[20,l] C. Z. Yuan,[1,46] Y. Yuan,[1] A. Yuncu,[45b,a] A. A. Zafar,[54] Y. Zeng,[20,l] B. X. Zhang,[1] B. Y. Zhang,[1,42] C. C. Zhang,[1] D. H. Zhang,[1] H. H. Zhang,[43] H. Y. Zhang,[1,42] J. Zhang,[1,46] J. L. Zhang,[58] J. Q. Zhang,[4] J. W. Zhang,[1,42,46] J. Y. Zhang,[1] J. Z. Zhang,[1,46] K. Zhang,[1,46] L. Zhang,[44] S. F. Zhang,[33] T. J. Zhang,[37,h] X. Y. Zhang,[36] Y. H. Zhang,[1,42] Y. T. Zhang,[52,42] Yan Zhang,[52,42] Yang Zhang,[1] Yao Zhang,[1] Yu Zhang,[46] Z. H. Zhang,[6] Z. P. Zhang,[52] Z. Y. Zhang,[57] G. Zhao,[1] J. W. Zhao,[1,42] J. Y. Zhao,[1,46] J. Z. Zhao,[1,42] Lei Zhao,[52,42] Ling Zhao,[1] M. G. Zhao,[34] Q. Zhao,[1] S. J. Zhao,[60] T. C. Zhao,[1] Y. B. Zhao,[1,42] Z. G. Zhao,[52,42] A. Zhemchugov,[27,b] B. Zheng,[53] J. P. Zheng,[1,42] W. J. Zheng,[36] Y. H. Zheng,[46] B. Zhong,[32] L. Zhou,[1,42]

Q. Zhou,[1,46] X. Zhou,[57] X. K. Zhou,[52,42] X. R. Zhou,[52,42] X. Y. Zhou,[1] A. N. Zhu,[1,46] J. Zhu,[34] K. Zhu,[1] K. J. Zhu,[1,42,46] S. Zhu,[1] S. H. Zhu,[51] X. L. Zhu,[44] Y. C. Zhu,[52,42] Y. S. Zhu,[1,46] Z. A. Zhu,[1,46] J. Zhuang,[1,42] B. S. Zou,[1] and J. H. Zou[1]

(BESIII Collaboration)

[1]*Institute of High Energy Physics, Beijing 100049, People's Republic of China*
[2]*Beihang University, Beijing 100191, People's Republic of China*
[3]*Beijing Institute of Petrochemical Technology, Beijing 102617, People's Republic of China*
[4]*Bochum Ruhr-University, D-44780 Bochum, Germany*
[5]*Carnegie Mellon University, Pittsburgh, Pennsylvania 15213, USA*
[6]*Central China Normal University, Wuhan 430079, People's Republic of China*
[7]*China Center of Advanced Science and Technology, Beijing 100190, People's Republic of China*
[8]*COMSATS University Islamabad, Lahore Campus, Defence Road, Off Raiwind Road, 54000 Lahore, Pakistan*
[9]*Fudan University, Shanghai 200443, People's Republic of China*
[10]*G.I. Budker Institute of Nuclear Physics SB RAS (BINP), Novosibirsk 630090, Russia*
[11]*GSI Helmholtzcentre for Heavy Ion Research GmbH, D-64291 Darmstadt, Germany*
[12]*Guangxi Normal University, Guilin 541004, People's Republic of China*
[13]*Guangxi University, Nanning 530004, People's Republic of China*
[14]*Hangzhou Normal University, Hangzhou 310036, People's Republic of China*
[15]*Helmholtz Institute Mainz, Johann-Joachim-Becher-Weg 45, D-55099 Mainz, Germany*
[16]*Henan Normal University, Xinxiang 453007, People's Republic of China*
[17]*Henan University of Science and Technology, Luoyang 471003, People's Republic of China*
[18]*Huangshan College, Huangshan 245000, People's Republic of China*
[19]*Hunan Normal University, Changsha 410081, People's Republic of China*
[20]*Hunan University, Changsha 410082, People's Republic of China*
[21]*Indian Institute of Technology Madras, Chennai 600036, India*
[22]*Indiana University, Bloomington, Indiana 47405, USA*
[23a]*INFN Laboratori Nazionali di Frascati, I-00044, Frascati, Italy*
[23b]*INFN and University of Perugia, I-06100, Perugia, Italy*
[24a]*INFN Sezione di Ferrara, I-44122, Ferrara, Italy*
[24b]*University of Ferrara, I-44122, Ferrara, Italy*
[25]*Institute of Physics and Technology, Peace Avenue 54B, Ulaanbaatar 13330, Mongolia*
[26]*Johannes Gutenberg University of Mainz, Johann-Joachim-Becher-Weg 45, D-55099 Mainz, Germany*
[27]*Joint Institute for Nuclear Research, 141980 Dubna, Moscow region, Russia*
[28]*Justus-Liebig-Universitaet Giessen, II. Physikalisches Institut, Heinrich-Buff-Ring 16, D-35392 Giessen, Germany*
[29]*KVI-CART, University of Groningen, NL-9747 AA Groningen, The Netherlands*
[30]*Lanzhou University, Lanzhou 730000, People's Republic of China*
[31]*Liaoning University, Shenyang 110036, People's Republic of China*
[32]*Nanjing Normal University, Nanjing 210023, People's Republic of China*
[33]*Nanjing University, Nanjing 210093, People's Republic of China*
[34]*Nankai University, Tianjin 300071, People's Republic of China*
[35]*Peking University, Beijing 100871, People's Republic of China*
[36]*Shandong University, Jinan 250100, People's Republic of China*
[37]*Shanghai Jiao Tong University, Shanghai 200240, People's Republic of China*
[38]*Shanxi University, Taiyuan 030006, People's Republic of China*
[39]*Sichuan University, Chengdu 610064, People's Republic of China*
[40]*Soochow University, Suzhou 215006, People's Republic of China*
[41]*Southeast University, Nanjing 211100, People's Republic of China*
[42]*State Key Laboratory of Particle Detection and Electronics, Beijing 100049, Hefei 230026, People's Republic of China*
[43]*Sun Yat-Sen University, Guangzhou 510275, People's Republic of China*
[44]*Tsinghua University, Beijing 100084, People's Republic of China*
[45a]*Ankara University, 06100 Tandogan, Ankara, Turkey*
[45b]*Istanbul Bilgi University, 34060 Eyup, Istanbul, Turkey*
[45c]*Uludag University, 16059 Bursa, Turkey*
[45d]*Near East University, Nicosia, North Cyprus, Mersin 10, Turkey*
[46]*University of Chinese Academy of Sciences, Beijing 100049, People's Republic of China*
[47]*University of Hawaii, Honolulu, Hawaii 96822, USA*

[48]University of Jinan, Jinan 250022, People's Republic of China
[49]University of Minnesota, Minneapolis, Minnesota 55455, USA
[50]University of Muenster, Wilhelm-Klemm-Straße 9, 48149 Muenster, Germany
[51]University of Science and Technology Liaoning, Anshan 114051, People's Republic of China
[52]University of Science and Technology of China, Hefei 230026, People's Republic of China
[53]University of South China, Hengyang 421001, People's Republic of China
[54]University of the Punjab, Lahore-54590, Pakistan
[55a]University of Turin, I-10125, Turin, Italy
[55b]University of Eastern Piedmont, I-15121, Alessandria, Italy
[55c]INFN, I-10125, Turin, Italy
[56]Uppsala University, P.O. Box 516, SE-75120 Uppsala, Sweden
[57]Wuhan University, Wuhan 430072, People's Republic of China
[58]Xinyang Normal University, Xinyang 464000, People's Republic of China
[59]Zhejiang University, Hangzhou 310027, People's Republic of China
[60]Zhengzhou University, Zhengzhou 450001, People's Republic of China

(Received 3 June 2019; revised manuscript received 25 August 2019; published 24 December 2019)

We study the reaction $e^+e^- \to \pi^+\pi^-\pi^0\eta_c$ for the first time using data samples collected with the BESIII detector at center-of-mass energies $\sqrt{s} = 4.226$, 4.258, 4.358, 4.416, and 4.600 GeV. Evidence of this process is found and the Born cross section $\sigma^B(e^+e^- \to \pi^+\pi^-\pi^0\eta_c)$, excluding $e^+e^- \to \omega\eta_c$ and $\eta\eta_c$, is measured to be $(46^{+12}_{-11} \pm 10)$ pb at $\sqrt{s} = 4.226$ GeV. Evidence for the decay $Z_c(3900)^\pm \to \rho^\pm\eta_c$ is reported at $\sqrt{s} = 4.226$ GeV with a significance of 3.9σ, including systematic uncertainties, and the Born cross section times branching fraction $\sigma^B(e^+e^- \to \pi^\mp Z_c(3900)^\pm) \times \mathcal{B}(Z_c(3900)^\pm \to \rho^\pm\eta_c)$ is measured to be $(48 \pm 11 \pm 11)$ pb, which indicates that $e^+e^- \to \pi^\mp Z_c(3900)^\pm \to \pi^\mp\rho^\pm\eta_c$ dominates the $e^+e^- \to \pi^+\pi^-\pi^0\eta_c$ process. The $Z_c(3900)^\pm \to \rho^\pm\eta_c$ signal is not significant at the other center-of-mass energies and the corresponding upper limits are determined. In addition, no significant signal is observed in a search for $Z_c(4020)^\pm \to \rho^\pm\eta_c$ with the same data samples. The ratios $R_{Z_c(3900)} = \mathcal{B}(Z_c(3900)^\pm \to \rho^\pm\eta_c)/\mathcal{B}(Z_c(3900)^\pm \to \pi^\pm J/\psi)$ and $R_{Z_c(4020)} = \mathcal{B}(Z_c(4020)^\pm \to \rho^\pm\eta_c)/\mathcal{B}(Z_c(4020)^\pm \to \pi^\pm h_c)$ are obtained and compared with different theoretical interpretations of the $Z_c(3900)^\pm$ and $Z_c(4020)^\pm$.

DOI: 10.1103/PhysRevD.100.111102

The charged charmonium-like states $Z_c(3900)^\pm$ [1–3] and $Z_c(4020)^\pm$ [4,5] were first observed in 2013. Although their observed properties indicate they are not conventional mesons consisting of a quark-antiquark pair, their exact quark configurations are still unknown. Several models have been developed to describe their inner structure [6], including loosely bound hadronic molecules of two charmed mesons [7], compact tetraquarks [8,9], and hadro-quarkonium [10,11].

It has recently been suggested that the relative decay rate of Z_c states, such as $Z_c(3900) \to \rho\eta_c$ to $\pi J/\psi$ [or $Z_c(4020) \to \rho\eta_c$ to πh_c], can be used to discriminate between the tetraquark and meson molecule scenarios [12]. In Ref. [12], the predicted ratio $R_{Z_c(3900)} = \mathcal{B}(Z_c(3900) \to \rho\eta_c)/\mathcal{B}(Z_c(3900) \to \pi J/\psi)$ is 230^{+330}_{-140} or $0.27^{+0.40}_{-0.17}$ based on the

[a]Also at Bogazici University, 34342 Istanbul, Turkey.
[b]Also at the Moscow Institute of Physics and Technology, Moscow 141700, Russia.
[c]Also at the Functional Electronics Laboratory, Tomsk State University, Tomsk, 634050, Russia.
[d]Also at the Novosibirsk State University, Novosibirsk, 630090, Russia.
[e]Also at the NRC "Kurchatov Institute," PNPI, 188300, Gatchina, Russia.
[f]Also at Istanbul Arel University, 34295 Istanbul, Turkey.
[g]Also at Goethe University Frankfurt, 60323 Frankfurt am Main, Germany.
[h]Also at Key Laboratory for Particle Physics, Astrophysics and Cosmology, Ministry of Education; Shanghai Key Laboratory for Particle Physics and Cosmology; Institute of Nuclear and Particle Physics, Shanghai 200240, People's Republic of China.
[i]Also at Key Laboratory of Nuclear Physics and Ion-beam Application (MOE) and Institute of Modern Physics, Fudan University, Shanghai 200443, People's Republic of China.
[j]Also at Harvard University, Department of Physics, Cambridge, Massachusetts 02138, USA.
[k]Also at State Key Laboratory of Nuclear Physics and Technology, Peking University, Beijing 100871, People's Republic of China.
[l]School of Physics and Electronics, Hunan University, Changsha 410082, China.

diquark-antidiquark tetraquark model, depending on how the spin-spin interaction outside the diquarks is treated. On the other hand, using nonrelativistic effective field theory techniques, this ratio is only $0.046^{+0.025}_{-0.017}$ if we assume the $Z_c(3900)$ is a meson molecule state. Similarly, the predicted ratio of $R_{Z_c(4020)} = \mathcal{B}(Z_c(4020) \to \rho\eta_c)/\mathcal{B}(Z_c(4020) \to \pi h_c)$ is $6.6^{+56.8}_{-5.8}$ in the tetraquark model, but only $0.010^{+0.006}_{-0.004}$ in the meson molecule model [12]. However, the well-separated predictions for $R_{Z(3900)}$ and $R_{Z(4020)}$, shown above, could move closer or even overlap according to different theoretical approaches. Within QCD sum rule approaches [13–16] and covariant quark model approaches [17] to the tetraquark scenario, the predicted value of $R_{Z_c(3900)}$ can vary from 0.66 to 1.86. Furthermore, different approaches to the meson molecule model [17–19] can lead to predictions for $R_{Z_c(3900)}$ from 6.8×10^{-3} to 1.8. Consequently, the capability to separate the molecular and tetraquark models is currently model dependent. In the hadron-charmonium model, the $Z_c(3900)$ is treated as a J/ψ embedded in an S-wave spinless excitation of light-quark matter and consequently the transition $Z_c(3900) \to \rho\eta_c$ is expected to be suppressed compared to $Z_c(3900) \to \pi J/\psi$. A search for the decays of $Z_c(3900)$ or $Z_c(4020)$ to $\rho\eta_c$ thus offers an important opportunity to discriminate among the wide range of theoretical predictions.

In this paper, we first report a search for the process $e^+e^- \to \pi^+\pi^-\pi^0\eta_c$. Then, based on the first step, we study the subprocesses $e^+e^- \to \pi Z_c(3900)^\pm$; $Z_c(3900)^\pm \to \rho^\pm\eta_c$ and $e^+e^- \to \pi Z_c(4020)^\pm$; $Z_c(4020)^\pm \to \rho^\pm\eta_c$. We use data samples collected with the BESIII detector [20] at center-of-mass (c.m.) energies above 4 GeV, as listed in Table I. The c.m. energies are measured using the $e^+e^- \to \mu^+\mu^-$ process with an uncertainty of ± 0.8 MeV [21]. The beam spread is measured to be 1.6 MeV.

The design and performance of the BESIII detector are given in Ref. [20]. A GEANT4-based [22] Monte Carlo (MC) simulation software package is used to optimize event selection criteria, determine the detection efficiencies, and estimate the backgrounds. At each energy, the signal events are generated according to phase space using EVTGEN [23]. Initial state radiation (ISR) is simulated with KKMC [24], and final state radiation is handled with PHOTOS [25].

Charged tracks, photons and K_S^0 candidates are reconstructed using the standard criteria of the BESIII experiment [26]. Candidate π^0 and η decays to $\gamma\gamma$ are reconstructed from pairs of photons with invariant mass in the range $[0.120, 0.145]$ GeV/c^2 for the π^0 and $[0.50, 0.57]$ GeV/c^2 for the η. To improve the resolution, a one-constraint (1C) kinematic fit is imposed on the selected photon pairs to constrain their invariant mass to the nominal π^0 or η mass [27].

The η_c candidates are reconstructed using nine hadronic decays: $p\bar{p}$, $2(K^+K^-)$, $K^+K^-\pi^+\pi^-$, $K^+K^-\pi^0$, $p\bar{p}\pi^0$, $K_S^0K^\pm\pi^\mp$, $\pi^+\pi^-\eta$, $K^+K^-\eta$, and $\pi^+\pi^-\pi^0\pi^0$. All combinations with invariant mass in the range $[2.7, 3.2]$ GeV/c^2 are kept within each event. The signal region for the η_c candidates is defined as $[2.95, 3.02]$ GeV/c^2 and the sidebands as [2.78, 2.92] and $[3.05, 3.19]$ GeV/c^2.

TABLE I. The Born cross section (σ^{B}) for the $e^+e^- \to \pi^+\pi^-\pi^0\eta_c$ process and the numbers that enter the calculation [see Eq. (1)]. Here, $\sqrt{s}$ is in GeV, $\mathcal{L}$ is in pb^{-1}, $\sum\epsilon\mathcal{B}$ is in % and σ^{B} is in pb.

$\sqrt{s}$	$\mathcal{L}$	N_{sig}	$(1+\delta)$	$\frac{1}{\lvert 1-\Pi\rvert^2}$	$\sum\epsilon\mathcal{B}$	$\sigma^{\mathrm{B}}(\sigma^{\mathrm{B}}_{\mathrm{U.L.}})$
4.226	1091.7	324^{+83}_{-80}	0.74	1.056	0.82	$46^{+12}_{-11} \pm 10$
4.258	825.7	157^{+73}_{-68}	0.76	1.054	0.80	$30^{+14}_{-13} \pm 9$ (<67)
4.358	539.8	32^{+62}_{-24}	1.03	1.051	0.62	$9^{+17}_{-7} \pm 2$ (<41)
4.416	1073.6	19^{+82}_{-18}	1.15	1.053	0.49	$3^{+13}_{-3} \pm 1$ (<38)
4.600	566.9	0^{+28}_{-0}	1.32	1.055	0.31	$0^{+12}_{-0} \pm 13$ (<36)

After the above selection, a four-constraint (4C) kinematic fit is performed for each event, and the χ^2 of the fit ($\chi^2_{4\mathrm{C}}$) is required to be less than 40 to suppress backgrounds. In each event, the mass of each track (excluding K_S^0 daughters) is taken to be that of the kaon, pion or proton, depending on the decay mode under study. Finally, only the combination of mass assignments with the minimum $\chi^2_{\mathrm{min}} \equiv \chi^2_{4\mathrm{C}} + \chi^2_{1\mathrm{C}} + \chi^2_{\mathrm{PID}} + \chi^2_{\mathrm{vertex}}$ is kept. Here, $\chi^2_{1\mathrm{C}}$ is the χ^2 of the 1C fit for π^0 (η), χ^2_{PID} is the sum of the χ^2 for the PID of all charged tracks, and χ^2_{vertex} is the χ^2 of the K_S^0 secondary vertex fit.

Inclusive MC samples with the same statistics as the data are studied to understand the backgrounds. The major backgrounds to $e^+e^- \to \pi^+\pi^-\pi^0\eta_c$ are classified into two categories. They are events from (1) charmonium(like) state decays (most of which include open-charm decays, e.g., $\psi \to D^{(*)}\bar{D}^{(*)}$); and (2) the continuum process, $e^+e^- \to q\bar{q}$, with $q = u$, d, and s.

By analyzing 600 000 $e^+e^- \to \pi^+\pi^-h_c$ MC simulation events with h_c decaying inclusively, a small enhancement in the η_c signal region is found. Using the measured cross section given in Ref. [4] and the luminosity of data, its contribution, $N^{\mathrm{peaking}}_{\mathrm{bkg}}$, is estimated to be 8.7 ± 2.0 at $\sqrt{s} = 4.226$ GeV. The contributions at other energies are estimated in a similar way.

To suppress background events with charmed mesons, events are rejected if a D meson candidate is reconstructed in one of its five decay modes: $D^0 \to K^\pm\pi^\mp$, $D^0 \to K^\pm\pi^\mp\pi^0$, $D^\pm \to K^\mp\pi^\pm\pi^\pm$, $D^\pm \to K_S^0\pi^\pm$, and $D^\pm \to K_S^0\pi^\pm\pi^0$. To accomplish this, we require the invariant mass of $D^0(D^\pm)$ candidates to be outside the region $m(D^0) \pm 24$ MeV $(m(D^\pm) \pm 10$ MeV). To reduce the continuum background, events with a $K^*(892) \to K\pi$, an $\omega \to \pi^+\pi^-\pi^0$, or an $\eta \to \pi^+\pi^-\pi^0$ candidate are removed by requiring $|M(K\pi) - m(K^*)| > 32$ MeV,

$|M(\pi^+\pi^-\pi^0) - m(\omega)| > 26$ MeV, and $|M(\pi^+\pi^-\pi^0) - m(\eta)| > 10$ MeV, respectively. Here, $m(D^0)$, $m(D^\pm)$, $m(K^*)$, $m(\omega)$ and $m(\eta)$ are the nominal masses of the corresponding states.

The mass windows for the background veto mentioned above and the χ^2 requirement of the 4C kinematic fit are determined by optimizing the figure-of-merit (FOM), which is defined as $\mathrm{FOM} = S/\sqrt{S+B}$. Here, S is the number of signal events from the MC simulation assuming $\sigma(e^+e^- \to \pi^+\pi^-\pi^0\eta_c) = 50$ pb, which is evaluated from a measurement with unoptimized selection criteria. B is the number of background events obtained from the η_c sidebands in the data and extrapolated to the signal region linearly. The optimization is performed through iterations until all the selection criteria become stable.

To obtain the $\pi^+\pi^-\pi^0\eta_c$ yield, the invariant mass distributions of the η_c candidates in the nine decay modes are fitted simultaneously using an unbinned maximum likelihood method. In the fit, the η_c signal shape is determined from MC simulation and is described with a constant-width Breit-Wigner function (mass and width are fixed to the world average values [27]) convolved with a Crystal Ball function, which represents instrumental resolution. The background is described with a second order Chebyshev polynomial (CP). Both the signal and background shapes are channel dependent, but the relative signal yields among all the channels are constrained by branching fractions and efficiencies [26]. The total signal yield of the nine channels is labeled N_{obs}, which is shared for all the channels and required to be positive. The free parameters in the fit include N_{obs} and the background yield and shape parameters for each decay mode. Figure 1 (left) shows the fit results at $\sqrt{s} = 4.226$ GeV projected onto the sum of events from all nine η_c decay modes. Figure 1 (right) shows the background-subtracted distribution. The total signal yield is 333^{+83}_{-80} with a statistical significance of 4.2σ, which is obtained by comparing the change of the log-likelihood value $\Delta(-\ln L) = 9.0$ with and without the $\pi^+\pi^-\pi^0\eta_c$ signal in the fit with 1 degree of freedom. The same selection criteria are applied to the other datasets, but no significant signals are observed.

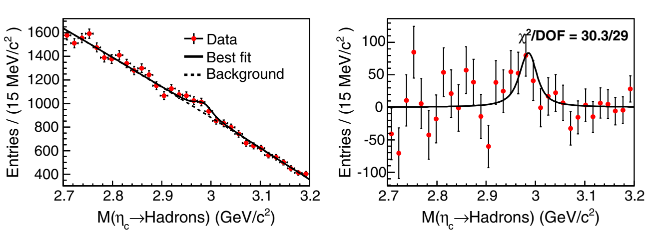

FIG. 1. Invariant mass distributions of the η_c candidates summed over nine channels in $e^+e^- \to \pi^+\pi^-\pi^0\eta_c$ at $\sqrt{s} = 4.226$ GeV (left panel), and the signal after background subtraction (right panel). Dots with error bars are the data, solid lines are the total fit, and the dotted line is background.

The Born cross section of the $e^+e^- \to \pi^+\pi^-\pi^0\eta_c$ reaction is calculated using

$$\sigma^{\mathrm{B}}(e^+e^- \to \pi^+\pi^-\pi^0\eta_c) = \frac{N_{\mathrm{sig}}}{\mathcal{L}(1+\delta)\frac{1}{|1-\Pi|^2}\sum_i \varepsilon_i \mathcal{B}_i}, \quad (1)$$

where $N_{\mathrm{sig}} = N_{\mathrm{obs}} - N_{\mathrm{bkg}}^{\mathrm{peaking}}$ is the number of signal events after the peaking background subtraction; $\mathcal{L}$ is the integrated luminosity; $(1+\delta)$ is the ISR correction factor, assuming the $\pi^+\pi^-\pi^0\eta_c$ signal is from $Y(4260)$ decays [27]; and $\frac{1}{|1-\Pi|^2}$ is the vacuum-polarization factor [28]. The cross sections and the numbers used for their calculation are listed in Table I for all energy points. The upper limits of the cross sections at 90% confidence level (C.L.) are determined using a Bayesian method, assuming a flat prior in σ^{B}. The systematic uncertainties are incorporated into the upper limit by smearing the probability density function of the cross section [26]. The corresponding results for $\sigma^{\mathrm{B}}_{\mathrm{U.L.}}$ are also listed in Table I.

The $Z_c(3900)^\pm$ and $Z_c(4020)^\pm$ signals are examined after requiring that the invariant mass of an η_c candidate is within the η_c signal region $[2.95, 3.02]$ GeV$/c^2$ and the invariant mass of $\pi^\pm\pi^0$ is within the ρ signal region $[0.675, 0.875]$ GeV$/c^2$. Here, we do not distinguish the pions from η_c decay or from collision and ρ decay, therefore all possible combinations in one event are kept to avoid bias. To suppress the combinatorial background, the momenta of the pions from the ρ decays are required to be less than 0.8 GeV$/c$. The events in the η_c sidebands and ρ sideband, which is defined as $[0.475, 0.675]$ GeV$/c^2$, are investigated and no peaking structure is found. In addition, the simulated background events are studied [Fig. 2 (left)] and show good agreement with data both in the η_c signal [Fig. 3 (top)] and sideband regions [Fig. 2 (right)]. In the data sample, the $Z_c(3900)^\pm$ signal is apparent, but there is no statistically significant $Z_c(4020)^\pm$ signal.

To obtain the yields of $e^+e^- \to \pi^\mp Z_c(3900)^\pm \to \pi^\mp\rho^\pm\eta_c$ and $e^+e^- \to \pi^\mp Z_c(4020)^\pm \to \pi^\mp\rho^\pm\eta_c$, the invariant mass of $\rho^\pm\eta_c$ candidates in the nine η_c decay channels are fitted

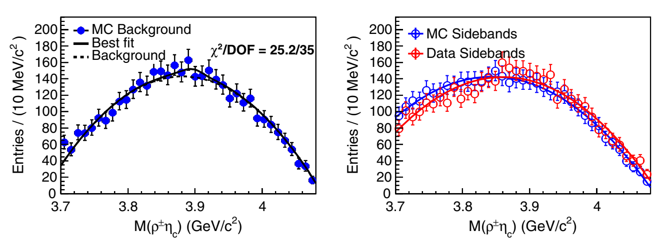

FIG. 2. Left: Fit to the simulated background at $\sqrt{s} = 4.226$ GeV in the η_c signal region. The black solid line is the best fit and dots with error bars are simulated background. Right: Fit to the sidebands in data and MC. The blue and red solid lines are the second order CP functions, the open blue and red dots with error bars are η_c sidebands in MC and data.

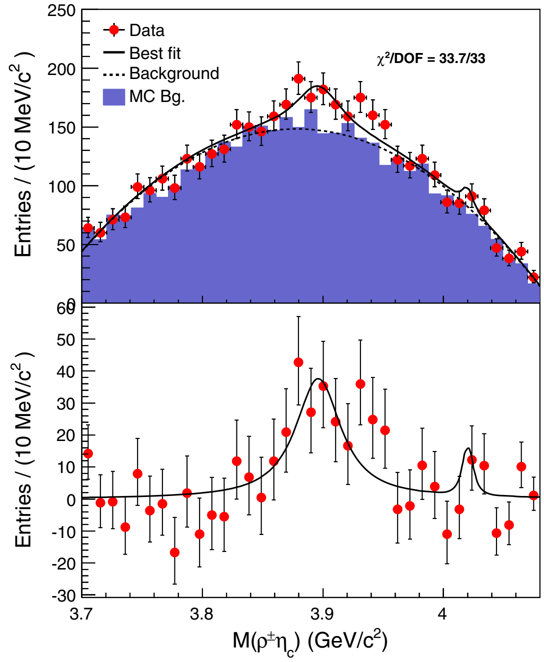

FIG. 3. The $\rho^{\pm}\eta_c$ invariant mass distribution summed over nine η_c decay channels in $e^+e^- \to \pi^{\mp}\rho^{\pm}\eta_c$ at $\sqrt{s} = 4.226$ GeV. Top: Dots with error bars are data and the shaded histogram is the simulated background. The solid line is the total fit and the dotted line is the background. Bottom: The same plot with the background subtracted.

simultaneously using the same method as for $e^+e^- \to \pi^+\pi^-\pi^0\eta_c$. In the fit, a possible interference between the signal and the background is neglected. The mass and width of the $Z_c(3900)^{\pm}$ are fixed to the values from the latest measurement [29] and those of the $Z_c(4020)^{\pm}$ are fixed to world average values [27]. The mass resolution is obtained from MC simulation and parametrized as a Crystal Ball function [30]. The background is described with a second order *CP* function. To validate the fit model, we perform a fit with the same model on the simulated background as shown in Fig. 2 (left). The signal yields of $Z_c(3900)^{\pm}$ and $Z_c(4020)^{\pm}$ are 48 ± 46 and 0 ± 4, respectively, and the statistical significance of the $Z_c(3900)^{\pm}$ is 0.6σ. We also fit the sideband events both from data and MC with the second order *CP* function and the function can describe the sidebands well as shown in Fig. 2 (right). After the validation, we apply the fit model to data. Figure 3 shows the fit to the dataset taken at $\sqrt{s} = 4.226$ GeV. The total $Z_c(3900)^{\pm}$ signal yield is 240^{+56}_{-54} events with a statistical significance of 4.3σ, and that of the $Z_c(4020)^{\pm}$ is 21^{+15}_{-11} events with a statistical significance of 1.0σ. The signals at the other c.m. energies are not statistically significant.

The Born cross section for $e^+e^- \to \pi^{\mp}Z_c^{\pm}$ with $Z_c^{\pm} \to \rho^{\pm}\eta_c$ is calculated using the same equation as shown in Eq. (1). The numbers used in the calculation and the results are listed in Table II.

The systematic uncertainties in the $\sigma^{\mathrm{B}}(e^+e^- \to \pi^+\pi^-\pi^0\eta_c)$ measurement originate from the uncertainty of each factor in Eq. (1). The integrated luminosity has an uncertainty of 1.0% [31]. The uncertainty due to the subtraction of the $e^+e^- \to \pi^+\pi^-h_c$ peaking background events includes both the uncertainty due to the cross section and the statistical error of the MC sample. To estimate the uncertainty due to ISR correction, the c.m. energy dependent cross section of $e^+e^- \to \pi^+\pi^-J/\psi$ measured by the BESIII experiment [32] is used instead of Y(4260). The uncertainty from the signal shape consists of the mass resolution discrepancy between data and MC simulation and the uncertainty of the η_c resonant parameters. The former is studied using an $e^+e^- \to \gamma_{ISR}J/\psi$ [33] sample and the latter is estimated by varying the η_c mass and width by $\pm 1\sigma$ around the world average values [27]. The uncertainty for the background shape is estimated by changing the order of the *CP* function and adjusting the fit boundaries. The methods for estimating the uncertainties due to the vacuum polarization and $\sum_i \epsilon_i \mathcal{B}_i$ are the same as those described in Ref. [26]. Furthermore, the uncertainty due to the $e^+e^- \to \pi^+\pi^-\pi^0\eta_c$ decay dynamics is obtained by comparing the simulations with and without the Z_c resonance. All of the sources are assumed to be independent and added in quadrature and the largest systematics uncertainty is that of $\sum_i \epsilon_i \mathcal{B}_i$. The total systematic uncertainties are listed in Table I.

TABLE II. Born cross sections of $e^+e^- \to \pi^{\mp}Z_c(3900)^{\pm} \to \pi^{\mp}\rho^{\pm}\eta_c$ and $e^+e^- \to \pi^{\mp}Z_c(4020)^{\pm} \to \pi^{\mp}\rho^{\pm}\eta_c$. $\mathcal{S}$ is the statistical significance of the signal. Other parameters are defined in the same way as those in Table I. Here, $Z_c(3900)$ is labeled as Z_c and $Z_c(4020)$ is labeled as Z'_c.

$\sqrt{s}$ (GeV)	$N^{Z_c}_{\mathrm{obs}}$	$N^{Z'_c}_{\mathrm{obs}}$	$(1+\delta)$	$\frac{1}{\lvert 1-\Pi\rvert^2}$	$\sum \epsilon^{Z_c}\mathcal{B}$ (%)	$\sum \epsilon^{Z'_c}\mathcal{B}$ (%)	$\sigma^{\mathrm{B}Z_c}$ (pb)	$\sigma^{\mathrm{B}Z_c}_{\mathrm{U.L.}}$	$\sigma^{\mathrm{B}Z'_c}_{\mathrm{U.L.}}$ (pb)	$\mathcal{S}^{Z_c}$ (σ)	$\mathcal{S}^{Z'_c}$ (σ)
4.226	240^{+56}_{-54}	21^{+15}_{-11}	0.74	1.056	0.59	0.52	$48^{+11}_{-11} \pm 11$	⋯	<14	4.3	1.0
4.258	92^{+48}_{-43}	0^{+11}_{-0}	0.76	1.054	0.50	0.56	$28^{+15}_{-13} \pm 8$	<62	<6	2.0	⋯
4.358	12^{+40}_{-8}	0^{+15}_{-0}	1.03	1.051	0.44	0.42	$5^{+16}_{-3} \pm 2$	<36	<14	0.3	⋯
4.416	101^{+48}_{-44}	6^{+17}_{-4}	1.15	1.053	0.35	0.34	$22^{+10}_{-10} \pm 5$	<44	<11	2.2	⋯
4.600	0^{+11}_{-0}	0^{+10}_{-0}	1.32	1.055	0.20	0.21	$0^{+7}_{-0} \pm 1$	<14	<21	⋯	⋯

For the $\sigma^B(e^+e^- \to \pi^\mp Z_c(3900)^\pm (Z_c(4020)^\pm) \to \pi^\mp\rho^\pm\eta_c)$ measurement, the uncertainties on $\mathcal{L}$, ISR factors, $\sum_i \varepsilon_i \mathcal{B}_i$ and the vacuum polarization factor are studied following the methods described in the measurement of $\sigma^B(e^+e^- \to \pi^+\pi^-\pi^0\eta_c)$. Moreover, additional systematic uncertainties arise from the ρ and η_c selections, and the fit of the invariant mass spectrum of $\rho^\pm\eta_c$. The uncertainty due to the $M(\pi^\pm\pi^0)$ mass window is estimated by comparing the invariant mass of $M(\omega \to \pi^+\pi^-\pi^0)$ in data and MC assuming the mass resolution of $M(\pi^+\pi^-\pi^0)$ is larger than $M(\pi^\pm\pi^0)$. The discrepancy is found to be negligible. The uncertainty of the η_c line shape is estimated by varying the mass and width of the η_c within the errors given by world average values [27]. The uncertainties affecting the fit to the $Z_c(3900)^\pm$ ($Z_c(4020)^\pm$) are estimated with the same methods as in the $\pi^+\pi^-\pi^0\eta_c$ case. All these sources and those in the $\sigma^B(e^+e^- \to \pi^+\pi^-\pi^0\eta_c)$ measurement are assumed to be independent and added in quadrature. The uncertainties related to the fit of invariant mass of $\eta_c \to$ hadrons are excluded because they do not affect the $e^+e^- \to \pi Z_c$ measurement. The largest systematics uncertainty comes from $\sum_i \varepsilon_i \mathcal{B}_i$. The total systematic uncertainties are listed in Table II.

To evaluate the effect of the systematic uncertainty on the signal significance at $\sqrt{s} = 4.226$ GeV, we vary the signal shape, background parametrization, and fit range, or free the Z_c mass, then repeat the fit. We find that the statistical significance of the $Z_c(3900)$ is always larger than 3.9σ.

In summary, using the e^+e^- annihilation data at $\sqrt{s} =$ 4.226, 4.258, 4.358, 4.416, and 4.600 GeV, we study the $e^+e^- \to \pi^+\pi^-\pi^0\eta_c$ process for the first time. Evidence of this process is observed at $\sqrt{s} = 4.226$ GeV with a significance of 4.2σ and the Born cross section $\sigma^B(e^+e^- \to \pi^+\pi^-\pi^0\eta_c)$ is measured to be $(46^{+12}_{-11} \pm 10)$ pb, excluding the processes $e^+e^- \to \omega\eta_c$ and $\eta\eta_c$. Evidence for the $\rho^\pm\eta_c$ decay mode of the charged charmonium-like state $Z_c(3900)^\pm$ is found in the process $e^+e^- \to \pi^\mp Z_c(3900)^\pm$ with $Z_c(3900)^\pm \to \rho^\pm\eta_c$ from the same dataset. The measured cross section times branching ratio $\sigma^B(e^+e^- \to \pi^\mp Z_c(3900)^\pm) \times \mathcal{B}(Z_c(3900)^\pm \to \rho^\pm\eta_c)$ is $(48 \pm 11 \pm 11)$ pb. This result indicates that the $e^+e^- \to \pi^+\pi^-\pi^0\eta_c$ process is dominated by the subprocess $e^+e^- \to \pi^\mp Z_c(3900)^\pm \to \pi^\mp\rho^\pm\eta_c$ [and implicitly $e^+e^- \to \pi^0 Z_c(3900)^0 \to \pi^0\rho^0\eta_c$]. The significance of $Z_c(3900)^\pm \to \rho^\pm\eta_c$ is 3.9σ including the systematical uncertainty. No significant signal of $e^+e^- \to \pi^+\pi^-\pi^0\eta_c$ is observed at $\sqrt{s} = 4.258$, 4.358, 4.416, and 4.600 GeV and no significant signal of $e^+e^- \to \pi^\mp Z_c(4020)^\pm$ with $Z_c(4020)^\pm \to \rho^\pm\eta_c$ is found in any of the datasets. Upper limits are determined at 90% C.L.

Using the results from Refs. [4,29], we calculate the ratios $R_{Z_c(3900)} = \mathcal{B}(Z_c(3900)^\pm \to \rho^\pm\eta_c)/\mathcal{B}(Z_c(3900)^\pm \to \pi^\pm J/\psi)$ and $R_{Z_c(4020)} = \mathcal{B}(Z_c(4020)^\pm \to \rho^\pm\eta_c)/\mathcal{B}(Z_c(4020)^\pm \to \pi^\pm h_c)$. The results obtained from the measurements at $\sqrt{s} = 4.226$, 4.258, and 4.358 GeV are listed in Table III, together with the theoretical predictions for comparison.

TABLE III. Comparison of the measured $R_{Z_c(3900)}$ and $R_{Z_c(4020)}$ with the theoretical predictions.

Ratio	Measurement	Tetraquark	Molecule
$R_{Z_c(3900)}$	2.3 ± 0.8 [29]	230^{+330}_{-140} [12]	$0.046^{+0.025}_{-0.017}$ [12]
		$0.27^{+0.40}_{-0.17}$ [12]	1.78 ± 0.41 [17]
		0.66 [13]	6.84×10^{-3} [18]
		0.56 ± 0.24 [14]	0.12 [19]
		0.95 ± 0.40 [15]	
		1.08 ± 0.88 [16]	
		1.28 ± 0.37 [17]	
		1.86 ± 0.41 [17]	
$R_{Z_c(4020)}$	<1.2 [4]	$6.6^{+56.8}_{-5.8}$ [12]	$0.010^{+0.006}_{-0.004}$ [12]

The measured $R_{Z_c(3900)}$ is closer to the calculation of the tetraquark model than to that of the meson molecule model in Ref. [12]. The measurement is also consistent with several other independent calculations based on the tetraquark scenario [13–17]. For the molecule model, as we mentioned before, the calculated $R_{Z_c(3900)}$ is highly model dependent [17–19]. Therefore, it is necessary to narrow down the theoretical uncertainty in the molecular framework to have a better comparison with the measurement. In the hadron-charmonium model, the $\mathcal{B}(Z_c(3900) \to \rho\eta_c)$ is suppressed compared with $\mathcal{B}(Z_c(3900) \to \pi J/\psi)$ and therefore inconsistent with the measurement [34]. Furthermore, this model predicts a new resonance $W_c(3785)$, which can be produced via $e^+e^- \to \rho W_c \to \rho\pi\eta_c$, the same final state we analyzed here. As we found that the $e^+e^- \to \pi^+\pi^-\pi^0\eta_c$ process is saturated by $e^+e^- \to \pi Z_c(3900) \to \rho\pi\eta_c$, we can conclude that the production of the W_c, if present, is small compared to $e^+e^- \to \pi Z_c(3900)$.

For $R_{Z_c(4020)}$, we can only report upper limits, but they are smaller than the value calculated based on the tetraquark model. On the other hand, the upper limits are not in contradiction with the molecule model calculation, which is about 2 orders of magnitude smaller than the current upper limits [12].

The BESIII collaboration thanks the staff of BEPCII and the IHEP computing center for their strong support. This work is supported in part by National Key Basic Research Program of China under Contract No. 2015CB856700; National Natural Science Foundation of China (NSFC) under Contracts No. 11335008, No. 11425524, No. 11625523, No. 11635010, No. 11735014, and No. 11575198; the Chinese Academy of Sciences (CAS) Large-Scale Scientific Facility Program; the CAS Center for Excellence in Particle Physics (CCEPP); Joint Large-Scale Scientific Facility Funds of the NSFC and CAS under Contracts No. U1532257, No. U1532258, and No. U1732263; CAS

Key Research Program of Frontier Sciences under Contracts No. QYZDJ-SSW-SLH003 and No. QYZDJ-SSW-SLH040; 100 Talents Program of CAS; INPAC and Shanghai Key Laboratory for Particle Physics and Cosmology; German Research Foundation DFG under Contracts Nos. Collaborative Research Center CRC 1044 and No. FOR 2359; Istituto Nazionale di Fisica Nucleare, Italy; Koninklijke Nederlandse Akademie van Wetenschappen (KNAW) under Contract No. 530-4CDP03; Ministry of Development of Turkey under Contract No. DPT2006K-120470; National Science and Technology fund; The Knut and Alice Wallenberg Foundation (Sweden) under Contract No. 2016.0157; The Swedish Research Council; U.S. Department of Energy under Contracts No. DE-FG02-05ER41374, No. DE-SC-0010118, and No. DE-SC-0012069; University of Groningen (RuG) and the Helmholtzzentrum fuer Schwerionenforschung GmbH (GSI), Darmstadt.

[1] M. Ablikim *et al.* (BESIII Collaboration), Phys. Rev. Lett. **110**, 252001 (2013).
[2] Z. Q. Liu *et al.* (Belle Collaboration), Phys. Rev. Lett. **110**, 252002 (2013).
[3] M. Ablikim *et al.* (BESIII Collaboration), Phys. Rev. Lett. **112**, 022001 (2014).
[4] M. Ablikim *et al.* (BESIII Collaboration), Phys. Rev. Lett. **111**, 242001 (2013).
[5] M. Ablikim *et al.* (BESIII Collaboration), Phys. Rev. Lett. **112**, 132001 (2014).
[6] For recent reviews, see H. X. Chen, W. Chen, X. Liu, and S. L. Zhu, Phys. Rep. **639**, 1 (2016); N. Brambilla *et al.*, Eur. Phys. J. C **71**, 1534 2011.
[7] M. B. Voloshin and L. B. Okun, Pis'ma Zh. Eksp. Teor. Fiz. **23**, 369 (1976) [JETP Lett. **23**, 333 (1976)]; http://www.jetpletters.ac.ru/ps/1801/article_27526.shtml.
[8] L. Maiani, F. Piccinini, A. D. Polosa, and V. Riquer, Phys. Rev. D **71**, 014028 (2005).
[9] Z. G. Wang and T. Huang, Phys. Rev. D **89**, 054019 (2014).
[10] M. B. Voloshin, Prog. Part. Nucl. Phys. **61**, 455 (2008).
[11] S. Dubynskiy and M. B. Voloshin, Phys. Lett. B **666**, 344 (2008).
[12] A. Esposito, A. L. Guerrieri, and A. Pilloni, Phys. Lett. B **746**, 194 (2015).
[13] L. Maiani, V. Riquer, R. Faccini, F. Piccinini, A. Pilloni, and A. D. Polosa, Phys. Rev. D **87**, 111102 (2013).
[14] S. S. Agaev, K. Azizi, and H. Sundu, Phys. Rev. D **93**, 074002 (2016).
[15] J. M. Dias, F. S. Navarra, M. Nielsen, and C. M. Zanetti, Phys. Rev. D **88**, 016004 (2013).
[16] Z. G. Wang and J. X. Zhang, Eur. Phys. J. C **78**, 14 (2018).
[17] F. Goerke, T. Gutsche, M. A. Ivanov, J. G. Korner, V. E. Lyubovitskij, and P. Santorelli, Phys. Rev. D **94**, 094017 (2016).
[18] S. Patel, M. Shah, K. Thakkar, and P. C. Vinodkumar, Proc. Sci., Hadron2013 (**2013**) 189.
[19] H. W. Ke, Z. T. Wei, and X. Q. Li, Eur. Phys. J. C **73**, 2561 (2013).
[20] M. Ablikim *et al.* (BESIII Collaboration), Nucl. Instrum. Methods Phys. Res., Sect. A **614**, 345 (2010).
[21] M. Ablikim *et al.* (BESIII Collaboration), Chin. Phys. C **40**, 063001 (2016).
[22] S. Agostinelli *et al.* (GEANT4 Collaboration), Nucl. Instrum. Methods Phys. Res., Sect. A **506**, 250 (2003).
[23] D. J. Lange, Nucl. Instrum. Methods Phys. Res., Sect. A **462**, 152 (2001).
[24] S. Jadach, B. F. L. Ward, and Z. Was, Comput. Phys. Commun. **130**, 260 (2000); Phys. Rev. D **63**, 113009 (2001).
[25] P. Golonka and Z. Was, Eur. Phys. J. C **45**, 97 (2006).
[26] M. Ablikim *et al.* (BESIII Collaboration), Phys. Rev. D **96**, 012001 (2017).
[27] M. Tanabashi *et al.* (Particle Data Group), Phys. Rev. D **98**, 030001 (2018).
[28] F. Jegerlehner, Z. Phys. C **32**, 195 (1986).
[29] M. Ablikim *et al.* (BESIII Collaboration), Phys. Rev. Lett. **119**, 072001 (2017).
[30] M. Oreglia, SLAC Report No. SLAC-236, 1980, p. 226.
[31] M. Ablikim *et al.* (BESIII Collaboration), Chin. Phys. C **39**, 093001 (2015).
[32] M. Ablikim *et al.* (BESIII Collaboration), Phys. Rev. Lett. **118**, 092001 (2017).
[33] M. Ablikim *et al.* (BESIII Collaboration), Phys. Rev. D **96**, 051101 (2017).
[34] M. B. Voloshin, Phys. Rev. D **87**, 091501 (2013).